Near-Forward Rescattering Photoelectron Holography in Strong-Field Ionization: Extraction of the Phase of the Scattering Amplitude

Yueming Zhou,[1,2] Oleg I. Tolstikhin,[3] and Toru Morishita[4,2]

[1]*School of Physics, Huazhong University of Science and Technology, Wuhan 430074, China*
[2]*Department of Engineering Science, The University of Electro-Communications, 1-5-1 Chofu-ga-oka, Chofu-shi, Tokyo 182-8585, Japan*
[3]*Moscow Institute of Physics and Technology, Dolgoprudny 141700, Russia*
[4]*Institute for Advanced Science, The University of Electro-Communications, 1-5-1 Chofu-ga-oka, Chofu-shi, Tokyo 182-8585, Japan*

(Received 6 October 2015; published 26 April 2016)

We revisit the concept of near-forward rescattering strong-field photoelectron holography introduced by Y. Huismans *et al.* [Science **331**, 61 (2011)]. The recently developed adiabatic theory is used to show how the phase of the scattering amplitude for near-forward rescattering of an ionized electron by the parent ion is encoded in and can be read out from the corresponding interference pattern in photoelectron momentum distributions (PEMDs) produced in the ionization of atoms and molecules by intense laser pulses. A procedure to extract the phase is proposed. Its application to PEMDs obtained by solving the time-dependent Schrödinger equation for a model atom yields results in good agreement with scattering calculations. This establishes a novel general approach to extracting structural information from strong-field observables capable of providing time-resolved imaging of ultrafast processes.

DOI: 10.1103/PhysRevLett.116.173001

An electron ionized from an atom or molecule by a strong laser field being driven by the field may return back and undergo rescattering by the parent ion [1,2]. This results in various processes such as elastic scattering [3,4], high-order harmonic generation [5], core excitation [6], multiple ionization [7], etc., constituting the subject of rapidly growing attosecond physics [8]. The goal is to extract structural information from the observable photoelectron and harmonic spectra, ultimately in a time-resolved manner. In recent years, a number of promising approaches to achieve this goal have been proposed [6,9–14]. In particular, it was shown theoretically [15] and demonstrated experimentally for atoms [16,17] and molecules [18] that the differential cross section for near-backward rescattering of an ionized electron by the parent ion can be accurately extracted from the photoelectron momentum distribution (PEMD). The experimental technique has been extended to time-resolved imaging of internuclear dynamics in molecules [19]. The differential cross section extracted from PEMDs in these experiments is given by the modulus of the electron-ion scattering amplitude squared [20]. In this Letter we propose a method that enables one to extract complementary structural information represented by the phase of the scattering amplitude in the near-forward direction. The observability of the phase of a scattering amplitude is known from the Mott scattering of identical particles [21]. The phase is fundamental for matter wave interferometry: in neutron [22] and atom or molecular [23] optics, electron-atom collisions [24], and particle physics [25]. Here, we reveal its presence in strong-field observables.

Strong-field PEMDs usually exhibit a rich interference structure determined by the different phases involved. The possibility to extract structural information from the phase-sensitive patterns in PEMDs is termed strong-field photoelectron holography (SFPEH), by analogy with optical holography [26]. The SFPEH pattern we are interested in was identified in a recent experiment with xenon [27] and then observed for other atoms [28–30] and molecules [31]. From the theoretical analysis in Ref. [27] it was recognized that this pattern results from the interference of electrons flying directly to the detector after tunneling ionization and those undergoing near-forward rescattering by the parent ion. It was also suggested that this pattern should encode some structural information [27,29,32], but what kind of information and how to decode it remained unknown. In this Letter we answer these most important questions.

We consider PEMDs produced in the ionization of an electron from a bound state in a central potential $V(r)$ by few-cycle pulses of an intense linearly polarized laser field $\mathbf{F}(t) = F(t)\mathbf{e}_z$, $F(\pm\infty) = 0$. We wish to demonstrate that they contain a general SFPEH pattern from which the phase of the amplitude of near-forward elastic scattering by the potential $V(r)$ can be extracted. Our analysis is based on the adiabatic theory [33], which is the asymptotics for $\epsilon \to 0$, where ϵ is the ratio of the atomic and laser field time scales. The solid mathematical foundation of this theory is confirmed by its good quantitative performance [33,34]. The PEMD in the adiabatic theory has the form $P(\mathbf{k}) = |I_a(\mathbf{k}) + I_r(\mathbf{k})|^2$, where $I_a(\mathbf{k})$ and $I_r(\mathbf{k})$ are the adiabatic and rescattering parts of the ionization amplitude, respectively, and $\mathbf{k} = (\mathbf{k}_\perp, k_z)$ is the photoelectron momentum. In leading order in ϵ, the adiabatic part is given by (atomic units are used throughout)

$$I_a(\mathbf{k}) = (2\pi)^{1/2} \sum_i \frac{A_0(k_\perp; t_{i0})}{|F(t_{i0})|^{1/2}} e^{i\mathcal{S}(t_{i0},\mathbf{k}) - is_0(t_{i0})}, \quad (1)$$

where

$$\mathcal{S}(t, \mathbf{k}) = \frac{1}{2} k_\perp^2 t + \frac{1}{2} \int_0^t [k_z - v_\infty + v(t')]^2 dt', \quad (2a)$$

$$s_0(t) = E_0 t + \int_{-\infty}^t [E_0(t') - E_0] dt', \quad (2b)$$

$v(t) = -\int_{-\infty}^t F(t')dt'$, and $v_\infty = v(\infty)$. Here, $E_0(t)$ is the energy of the Siegert (outgoing-wave) state originating from the initial bound state with energy $E_0 = E_0(\pm\infty)$ in the presence of a static electric field equal to the instantaneous value of $F(t)$ and $A_0(k_\perp; t)$ is the transverse momentum distribution amplitude in this state [33,35]. The summation in Eq. (1) runs over the different ionization moments $t_{i0} = t_{i0}(k_z)$ defined by

$$k_z - v_\infty + v(t_{i0}) = 0. \quad (3)$$

The rescattering part is given by

$$I_r(\mathbf{k}) = (2\pi)^{1/2} \sum_{ir} \frac{A_0(0; t_i) f(p, \theta)}{|(t_r - t_i)^3 F(t_i) S_r''|^{1/2}} \times e^{i\mathcal{S}(t_r,\mathbf{k}) - i\mathcal{S}(t_r,t_i) - is_0(t_i)}, \quad (4)$$

where

$$\mathcal{S}(t_r, t_i) = \frac{1}{2} \int_{t_i}^{t_r} [v(t) - v(t_i)]^2 dt. \quad (5)$$

Here, $f(p, \theta)$ is the scattering amplitude for the potential $V(r)$ at the incident momentum $p = |u_f|$ and scattering angle $\theta = \arccos([k_z - v_\infty + v(t_r)]/u_f)$, where $u_f = v(t_r) - v(t_i)$ and $S_r'' = -F(t_r)[k_z - v_\infty + v(t_i)] + u_f^2/(t_r - t_i)$. The summation in Eq. (4) runs over the different pairs of the ionization $t_i = t_i(k_\perp, k_z)$ and rescattering $t_r = t_r(k_\perp, k_z)$ moments defined by

$$(t_r - t_i) v(t_i) = \int_{t_i}^{t_r} v(t) dt, \quad (6a)$$

$$[v(t_r) - v(t_i)]^2 = k_\perp^2 + [k_z - v_\infty + v(t_r)]^2. \quad (6b)$$

For brevity, some phase factor common for all terms in Eqs. (1) and (4) is omitted.

The transverse component $\mathbf{k}_\perp$ of the photoelectron momentum in Eqs. (1) and (4) has different origins. In the adiabatic part (1), an electron is ionized at time t_{i0} with the initial momentum $\mathbf{k}_\perp$; Eq. (3) means that its initial momentum along the field is zero. The distribution of the ionized electrons in $\mathbf{k}_\perp$ is determined by the transverse momentum distribution amplitude $A_0(k_\perp; t_{i0})$, which accounts for the interaction with the parent ion during tunneling ionization. Their motion after ionization is driven only by the field; the interaction with the parent ion causing rescattering appears only in the next order in ϵ, so the distribution in $\mathbf{k}_\perp$ remains unchanged. The rescattering part (4) accounts for the latter interaction. Here, an electron is ionized at time t_i with zero initial momentum. Being driven by the field, it returns to the parent ion at time t_r with momentum $u_f \mathbf{e}_z$. As a result of rescattering, its momentum acquires the transverse component $\mathbf{k}_\perp$, with Eq. (6b) ensuring the conservation of energy in the rescattering event. For forward rescattering $\theta = 0$, $k_\perp = 0$, and $k_z - v_\infty + v(t_i) = 0$. As seen from Eqs. (3) and (6), in this case $t_{i0}(k_z) = t_i(0, k_z)$. Thus, the same collinear classical trajectory determines both the adiabatic and rescattering contributions; let $t_{r0}(k_z) = t_r(0, k_z)$ denote the moment of rescattering for this trajectory. In the adiabatic regime $t_{r0} - t_{i0} = O(\epsilon^{-1})$, $|u_f| = O(\epsilon^{-1})$, and the PEMD is localized in the region $k_\perp = O(\epsilon^0)$ and $k_z = O(\epsilon^{-1})$ [33]. Then the solutions to Eqs. (6) can be divided into two groups corresponding to either near-forward, $\theta = O(\epsilon^1)$, or near-backward, $\pi - \theta = O(\epsilon^1)$, rescattering. We are interested only in the former case. In this case Eqs. (6) have a solution (t_i, t_r) located at a distance $O(\epsilon^1)$ from (t_{i0}, t_{r0}). This establishes a correspondence between the adiabatic (direct) terms in Eq. (1) and the near-forward rescattering terms in Eq. (4) contributing to the PEMD at the same $\mathbf{k}$. Let us pick up one pair of the corresponding terms, denoting them by $I_a^{(i)}$ and $I_r^{(i)}$. They act as the reference and object waves in optical holography [26], respectively. Their interference produces the SFPEH in focus here. The corresponding pattern in the PEMD is easily distinguishable from the other interference structures caused by the different terms in Eqs. (1) and (4) and can be considered separately. We have

$$|I_a^{(i)} + I_r^{(i)}|^2 = |I_a^{(i)}|^2 + |I_r^{(i)}|^2 + 2|I_a^{(i)} I_r^{(i)}| \cos \Delta\phi_{\mathrm{AA}}, \quad (7)$$

where $\Delta\phi_{\mathrm{AA}}$ is the difference of the phases of $I_a^{(i)}$ and $I_r^{(i)}$. By expanding this interference phase in ϵ we obtain

$$\Delta\phi_{\mathrm{AA}} = \frac{1}{2} k_\perp^2 (t_{r0} - t_{i0}) + \alpha + O(\epsilon^1), \quad (8)$$

where α is the phase of the scattering amplitude $f(p, \theta) = |f(p, \theta)| e^{i\alpha(p,\theta)}$. The first and second terms on the right-hand side of Eq. (8) have orders $O(\epsilon^{-1})$ and $O(\epsilon^0)$, respectively; we emphasize that no other terms appear in Eq. (8) in the specified orders in ϵ. The first term has a classical origin and was discussed in Refs. [27,28,32]. The second quantum term α plays the key role in the present analysis; as far as we know, it has not appeared in the literature. Thus, the adiabatic theory [33] predicts that strong-field PEMDs contain an interference pattern determined by the phase (8). The structural information represented by $\alpha(p, \theta)$ in the region of its arguments as functions of $(k_\perp, k_z)$ covered by the PEMD is encoded in this pattern and can be extracted from it.

Let us show that this is indeed the case. The adiabatic theory is currently developed only for potentials without a Coulomb tail. To stay within the region of applicability of the theory, we illustrate our analysis by calculations for a screened Coulomb potential

$$V(r) = -\exp[-(r/a)^2]/r. \qquad (9)$$

The dependence on the target is illustrated by considering two values of the screening parameter, $a = 10$ and 20. In both cases, the initial state is the ground $1s$ state with energy $E_0 \approx -0.4855$ and -0.4963, respectively. The PEMDs are obtained by solving the time-dependent Schrödinger equation (TDSE) using a method developed in Ref. [36]. We first consider a one-cycle pulse defined by $F(t) = -\sqrt{2e}F_0(2t/\tau)e^{-(2t/\tau)^2}$ with the amplitude $F_0 = \max[F(t)] = 0.1$ (corresponding to the intensity of 3.5×10^{14} W/cm^2) and duration $\tau = 75$ ($\lambda \approx 800$ nm). For this pulse there exist only two direct terms in Eq. (1) originating from each of the two half cycles and only the first of them has a near-forward rescattering counterpart in Eq. (4) [33], which makes the interference structure of the PEMD especially simple. The PEMD for this pulse calculated with $a = 10$ is shown in Fig. 1(a). One can see two types of interference fringes. The nearly vertical high-contrast ones result from the interference of the two direct contributions in Eq. (1). These fringes are well known theoretically [37,38], but are usually not observable experimentally (with a few important exceptions [39–41]) because their position depends on the intensity and they are averaged out in the integrated signal from the laser focal volume. The less pronounced nearly horizontal fringes are caused by the interference of the first direct and the corresponding near-forward rescattering contributions in Eqs. (1) and (4). This is the SFPEH we are interested in. A similar holographic pattern was observed experimentally in Refs. [27–31]; the conditions of its visibility were analyzed in Ref. [42].

To make the horizontal fringes more visible, we apply the following two-step procedure to the raw TDSE results. First, we eliminate the vertical fringes by averaging the PEMD over k_z in an interval $k_z \pm \Delta k_z$ of a suitable width $2\Delta k_z$. Cuts of the thus obtained averaged PEMDs for the potential (9) with $a = 10$ and 20 taken at $k_z = 2.2$ as functions of $k_\perp$ are shown in Fig. 2(a). For comparison, we also show the results obtained for the Coulomb potential, $a = \infty$. The horizontal fringes are seen as modulations of the cuts. Second, we fit the cuts by the function

$$e^{-f(k_\perp)}[1 + g(k_\perp)\cos\Delta\phi_{\mathrm{TDSE}}] \qquad (10)$$

whose form is suggested by Eq. (7). Here, $f(k_\perp)$ describes a monotonically decreasing background contribution and is determined by fitting the logarithm of the averaged PEMD by

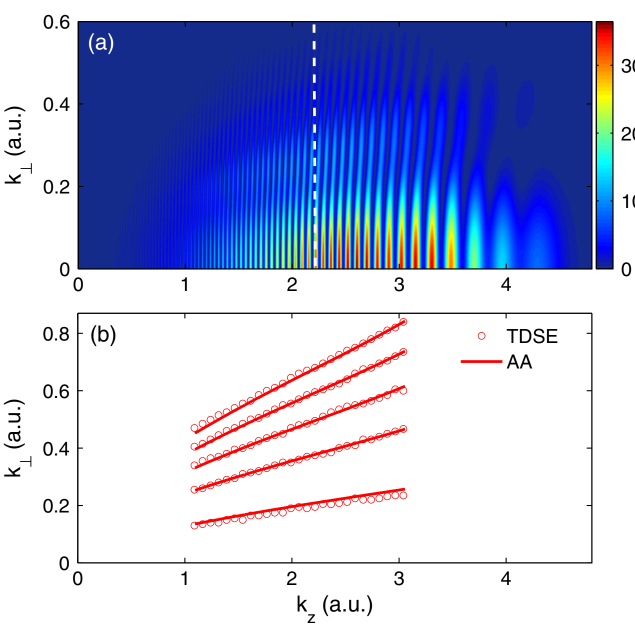

FIG. 1. (a) TDSE results for the PEMD produced in the ionization of a model atom described by the potential (9) with $a = 10$ by a one-cycle pulse with $\lambda \approx 800$ nm and the intensity of 3.5×10^{14} W/cm^2. (b) Open circles: interference minima of the near-forward rescattering SFPEH extracted from the TDSE results using a procedure described in the text. Solid lines: positions of the minima in the adiabatic approximation found from $\Delta\phi_{\mathrm{AA}} = (2n+1)\pi$, with $n = 0, 1, \ldots, 4$ and $\Delta\phi_{\mathrm{AA}}$ given by Eq. (8).

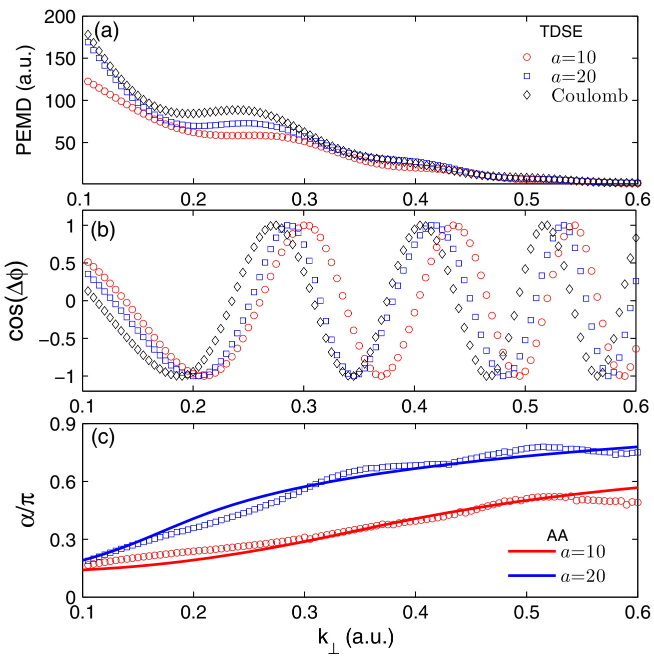

FIG. 2. (a) Cuts of the PEMDs calculated for the potential (9) with $a = 10$ (red circles) and $a = 20$ (blue squares) and for the Coulomb potential (black diamonds) and averaged over k_z in the interval $k_z = 2.2 \pm 0.1$ near the vertical dashed line in Fig. 1(a) as functions of $k_\perp$. (b) The function $\cos\Delta\phi_{\mathrm{TDSE}}$ extracted by fitting the results in panel (a) by Eq. (10). (c) The phase α of the scattering amplitude extracted from the results in panel (b) using $\Delta\phi_{\mathrm{TDSE}} = \Delta\phi_{\mathrm{AA}}$ and Eq. (8) (symbols) and obtained from scattering calculations (solid lines).

a polynomial. Dividing the fitted function by $e^{-f(k_\perp)}$ and subtracting unity, we obtain an oscillating function with a smooth envelope $g(k_\perp)$, which is again fitted by a polynomial. By construction, the remaining factor $\cos\Delta\phi_{\rm TDSE}$ is bounded between -1 and $+1$. This factor is shown in Fig. 2(b). The calculations can be repeated for the different values of k_z. They yield stable results independent of the details of the fitting procedure at intermediate k_z not very close to the classical boundaries of the PEMD [33] (at $k_z = 0$ and 4.37 for the present pulse). The minima of the thus extracted factor $\cos\Delta\phi_{\rm TDSE}$ as functions of k_z for the potential with $a = 10$ are shown by open circles in Fig. 1(b). Their positions nicely agree with the predictions of the adiabatic theory (8) shown by solid lines. This confirms the equality $\Delta\phi_{\rm TDSE} = \Delta\phi_{\rm AA}$ expected in the adiabatic approximation. The phase α extracted from this equality for $a = 10$ and 20 at $k_z = 2.2$ as a function of $k_\perp$ is shown by symbols in Fig. 2(c). For both potentials, its values are in good agreement with the results of scattering calculations shown by the solid lines. This establishes a procedure to extract α from a PEMD by means of Eqs. (8) and (10).

Although the results for finite a in Figs. 2(a) and 2(b) seem to converge to the Coulomb results as a grows, Eq. (8) does not apply in the Coulomb case, which explains the absence of the Coulomb results in Fig. 2(c). This is because Eqs. (1) and (4) were derived under the condition that the range a of the potential does not exceed the amplitude $F_0/\omega^2 = O(\epsilon^{-2})$ of oscillations of a free electron in the laser field [33]. For any finite a this condition can be satisfied by decreasing the frequency $\omega = O(\epsilon^1)$. As follows from Eq. (8), at the first interference fringe of the SFPEH pattern we have $\theta \sim k_\perp/|u_f| = O(\epsilon^{3/2})$. The pattern lies at larger θ. Scattering at such angles probes the potential at $r < O(\epsilon^{-3/2})$, which is within the region of validity of Eq. (8). Thus, the adiabatic theory fully covers the inner region of the potential determining the phase of the scattering amplitude extracted, with the important structural information encoded, and only the extreme Coulomb tail corresponding to very small θ at the edge of the SFPEH pattern remains not accounted for.

We next demonstrate that the near-forward rescattering SFPEH pattern survives and the extraction procedure still works for more realistic pulse shapes. We now consider a few-cycle pulse with $F(t) = -F_0\cos(2\pi t/T)e^{-(t/\tau)^2}$, where again $F_0 = 0.1$, $T = 165$ is the laser period ($\lambda \approx 1200$ nm), and $\tau = T/\sqrt{2\ln 2}$, see Fig. 3(a). The PEMD for this pulse calculated for the potential with $a = 10$ is shown in Fig. 3(b). The horizontal interference fringes of the type discussed above are seen at negative k_z. They present a hologram produced by electrons ionized during the quarter cycle $0 < t < T/4$ following the main maximum of $|F(t)|$ at $t = 0$; the other maxima of the field produce less pronounced interference patterns. We use the same averaging and fitting procedure to extract the phase α of the scattering amplitude; the results are shown in Fig. 3(c). The results of scattering calculations of the phase

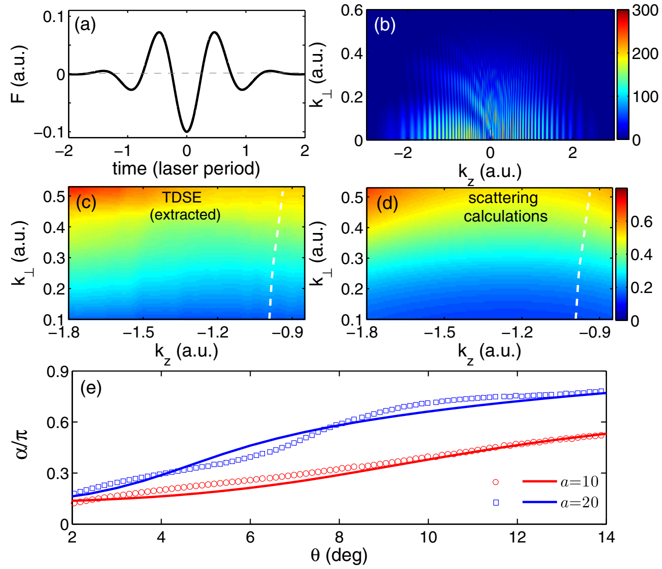

FIG. 3. (a) The electric field of a few-cycle pulse with $\lambda \approx 1200$ nm and the intensity of 3.5×10^{14} W/cm^2. (b) The PEMD produced by this pulse calculated for the potential (9) with $a = 10$. (c) The phase α (in units of π) of the scattering amplitude extracted from the results in panel (b). (d) The same phase obtained from scattering calculations. (e) The extracted (symbols) and calculated (solid lines) phase $\alpha(p,\theta)$ at a fixed incident momentum $p = 2.1$ as a function of the scattering angle θ taken along the white dashed lines in panels (c) and (d), respectively, for the potentials with $a = 10$ and 20.

are shown in Fig. 3(d). The agreement is good in a wide region of the photoelectron momentum $(k_\perp, k_z)$. This region maps onto a region of the incident momentum p and scattering angle θ, which enables one to obtain the phase $\alpha(p,\theta)$ as a function of its conventional arguments. For example, along the white dashed lines in Figs. 3(c) and 3(d) we have $p = 2.1$. The extracted values of $\alpha(p = 2.1, \theta)$ for the two potentials are shown by symbols in Fig. 3(e). They are in good agreement with the results of the scattering calculations shown by the solid lines. Note that the extracted structural information is rather sensitive to the target and even the relatively small difference between the two potentials considered is clearly resolved.

It is important to mention that the phase α encoded in the SFPEH pattern is read out at time $t_r - t_i \approx t_{r0} - t_{i0}$ after ionization. This time depends on k_z, and hence α as a function of $k_\perp$ extracted at different k_z corresponds to different times. This means that the structural information contained in the values of α extracted from a PEMD provides a time-resolved imaging of the target dynamics. Such a possibility was recognized in Ref. [27].

Summarizing, we have revisited the concept of near-forward rescattering SFPEH [27] on the basis of the adiabatic theory [33]. The corresponding interference pattern in PEMDs is a robust feature that exists for different targets and laser pulses and survives focal volume averaging, as confirmed by its experimental observations for atoms [27–30] and molecules [31]. We have shown that this pattern encodes the phase of the scattering amplitude for near-forward rescattering of an ionized electron by the parent ion. A procedure to extract the phase from PEMDs is proposed; its results are shown to be in good agreement with scattering calculations and sensitive to the target structure. This establishes a novel general approach to extracting structural information from strong-field observables capable of providing time-resolved imaging of ultrafast processes in the attosecond regime.

This work was supported in part by JSPS KAKENHI Grants No. 26400415 and No. 10500598. O. I. T. acknowledges support from the Ministry of Education and Science of Russia (State Assignment No. 3.679.2014/K). T. M. was supported in part by the RFBR-JSPS Bilateral Joint Research program.

[1] K. J. Schafer, B. Yang, L. F. DiMauro, and K. C. Kulander, Phys. Rev. Lett. **70**, 1599 (1993).

[2] P. B. Corkum, Phys. Rev. Lett. **71**, 1994 (1993).

[3] B. Yang, K. J. Schafer, B. Walker, K. C. Kulander, P. Agostini, and L. F. DiMauro, Phys. Rev. Lett. **71**, 3770 (1993).

[4] G. G. Paulus, W. Nicklich, H. Xu, P. Lambropoulos, and H. Walther, Phys. Rev. Lett. **72**, 2851 (1994).

[5] M. Ferray, A. L'Huillier, X. F. Li, L. A. Lomprk, G. Mainfray, and C. Manus, J. Phys. B **21**, L31 (1988).

[6] H. Niikura, F. Légaré, R. Hasbani, A. D. Bandrauk, M. Y. Ivanov, D. M. Villeneuve, and P. B. Corkum, Nature (London) **417**, 917 (2002).

[7] B. Walker, B. Sheehy, L. F. DiMauro, P. Agostini, K. J. Schafer, and K. C. Kulander, Phys. Rev. Lett. **73**, 1227 (1994).

[8] F. Krausz and M. Ivanov, Rev. Mod. Phys. **81**, 163 (2009).

[9] J. Itatani, J. Levesque, D. Zeidler, H. Niikura, H. Pépin, J. C. Kieffer, P. B. Corkum, and D. M. Villeneuve, Nature (London) **432**, 867 (2004).

[10] S. Baker, J. S. Robinson, C. A. Haworth, H. Teng, R. A. Smith, C. C. Chirilă, M. Lein, J. W. G. Tisch, and J. P. Marangos, Science **312**, 424 (2006).

[11] M. Meckel, D. Comtois, D. Zeidler, A. Staudte, D. Pavičić, H. C. Bandulet, H. Pépin, J. C. Kieffer, R. Dörner, D. M. Villeneuve, and P. B. Corkum, Science **320**, 1478 (2008).

[12] W. Li, X. Zhou, R. Lock, S. Patchkovskii, A. Stolow, H. C. Kapteyn, and M. M. Murnane, Science **322**, 1207 (2008).

[13] H. Wörner, J. Bertrand, D. Kartashov, P. Corkum, and D. Villeneuve, Nature (London) **466**, 604 (2010).

[14] P. M. Kraus, O. I. Tolstikhin, D. Baykusheva, A. Rupenyan, J. Schneider, C. Z. Bisgaard, T. Morishita, F. Jensen, L. B. Madsen, and H. J. Wörner, Nat. Commun. **6**, 7039 (2015).

[15] T. Morishita, A.-T. Le, Z. Chen, and C. D. Lin, Phys. Rev. Lett. **100**, 013903 (2008).

[16] M. Okunishi, T. Morishita, G. Prümper, K. Shimada, C. D. Lin, S. Watanabe, and K. Ueda, Phys. Rev. Lett. **100**, 143001 (2008).

[17] D. Ray, B. Ulrich, I. Bocharova, C. Maharjan, P. Ranitovic, B. Gramkow, M. Magrakvelidze, S. De, I. V. Litvinyuk, A.-T. Le, T. Morishita, C. D. Lin, G. G. Paulus, and C. L. Cocke, Phys. Rev. Lett. **100**, 143002 (2008).

[18] C. Wang, M. Okunishi, R. R. Lucchese, T. Morishita, O. I. Tolstikhin, L. B. Madsen, K. Shimada, D. Ding, and K. Ueda, J. Phys. B **45**, 131001 (2012).

[19] C. I. Blaga, J. Xu, A. D. DiChiara, E. Sistrunk, K. Zhang, P. Agostini, T. A. Miller, L. F. DiMauro, and C. D. Lin, Nature (London) **483**, 194 (2012).

[20] R. G. Newton, *Scattering Theory of Waves and Particles* (Springer-Verlag, New York, 1982).

[21] N. F. Mott, Proc. R. Soc. A **126**, 259 (1930).

[22] V. F. Sears, *Neutron Optics* (Oxford University Press, Oxford, 1990).

[23] J. Schmiedmayer, M. S. Chapman, C. R. Ekstrom, T. D. Hammond, S. T. Wehinger, and D. E. Pritchard, Phys. Rev. Lett. **74**, 1043 (1995).

[24] R. C. Forrey, A. Dalgarno, and J. Schmiedmayer, Phys. Rev. A **59**, R942 (1999).

[25] I. P. Ivanov, Phys. Rev. D **85**, 076001 (2012).

[26] D. Gabor, Nature (London) **161**, 777 (1948).

[27] Y. Huismans *et al.*, Science **331**, 61 (2011).

[28] Y. Huismans *et al.*, Phys. Rev. Lett. **109**, 013002 (2012).

[29] D. D. Hickstein, P. Ranitovic, S. Witte, X.-M. Tong, Y. Huismans, P. Arpin, X. Zhou, K. E. Keister, C. W. Hogle, B. Zhang, C. Ding, P. Johnsson, N. Toshima, M. J. J. Vrakking, M. M. Murnane, and H. C. Kapteyn, Phys. Rev. Lett. **109**, 073004 (2012).

[30] D. G. Arbó, C. Lemell, S. Nagele, N. Camus, L. Fechner, A. Krupp, T. Pfeifer, S. D. López, R. Moshammer, and J. Burgdörfer, Phys. Rev. A **92**, 023402 (2015).

[31] M. Meckel, A. Staudte, S. Patchkovskii, D. M. Villeneuve, P. B. Corkum, R. Dörner, and M. Spanner, Nat. Phys. **10**, 594 (2014).

[32] X.-B. Bian, Y. Huismans, O. Smirnova, K.-J. Yuan, M. J. J. Vrakking, and A. D. Bandrauk, Phys. Rev. A **84**, 043420 (2011).

[33] O. I. Tolstikhin and T. Morishita, Phys. Rev. A **86**, 043417 (2012).

[34] M. Ohmi, O. I. Tolstikhin, and T. Morishita, Phys. Rev. A **92**, 043402 (2015).

[35] P. A. Batishchev, O. I. Tolstikhin, and T. Morishita, Phys. Rev. A **82**, 023416 (2010).

[36] T. Morishita, Z. Chen, S. Watanabe, and C. D. Lin, Phys. Rev. A **75**, 023407 (2007).

[37] D. G. Arbó, E. Persson, and J. Burgdörfer, Phys. Rev. A **74**, 063407 (2006).

[38] D. G. Arbó, K. L. Ishikawa, K. Schiessl, E. Persson, and J. Burgdörfer, Phys. Rev. A **81**, 021403(R) (2010).

[39] F. Lindner, M. G. Schätzel, H. Walther, A. Baltuška, E. Goulielmakis, F. Krausz, D. B. Milošević, D. Bauer, W. Becker, and G. G. Paulus, Phys. Rev. Lett. **95**, 040401 (2005).

[40] X. Xie, S. Roither, D. Kartashov, E. Persson, D. G. Arbó, L. Zhang, S. Gräfe, M. S. Schöffler, J. Burgdörfer, A. Baltuška, and M. Kitzler, Phys. Rev. Lett. **108**, 193004 (2012).

[41] M. Richter, M. Kunitski, M. Schöffler, T. Jahnke, L. P. H. Schmidt, M. Li, Y. Liu, and R. Dörner, Phys. Rev. Lett. **114**, 143001 (2015).

[42] T. Marchenko, Y. Huismans, K. J. Schafer, and M. J. J. Vrakking, Phys. Rev. A **84**, 053427 (2011).